Determination of Elastic and Thermal Properties of Nanocomposites by Fiber Embedment in Finite Elements

P.D. Spanos[*], M. Esteva[**] and J.E. Akin[**]

[*] L.B. Ryon Chair in Engineering, Rice University MS-321, Houston, TX, 77251-1982, United States, Tel: +1 713 348 4909, fax: +1 713 348 5191, email: spanos@rice.edu
[**] Department of Mechanical Engineering and Material Science, Rice University MS-321, Houston, TX, 77251-1892, United States

ABSTRACT

In this paper the effect of entangled and non-straight fibers on the values of the effective elastic and thermal properties of polymer nanocomposite (PNC) is addressed. Most of the models in recent studies assume nanotubes to be well dispersed straight fibers with fixed size. Experiments also reveal that nanotubes become wavy during the manufacturing process, due to their high aspect ratio and low bending stiffness. Furthermore, experiments also show that nanotubes come in a variety of diameters and lengths. In the paper an attempt to predict the properties of composites with entangled nanotubes is made in which the distributions regarding the nanotube length and diameter are incorporated. First, an approach to generate random microstructures is developed. Then, using the embedded fiber finite element method (EFFEM), the effective properties are computed for each of the random microstructures. This approach requires only a regular grid for the finite element (FE) mesh, circumventing the computationally costly and human labor intensive mesh refinement of ordinary FE required for capturing the local morphology of the composite material. Finally, a Monte Carlo (MC) simulation approach is used to obtain statistics of the computed effective physical properties. The numerical results are found in good agreement with experimental data reported in the open literature.

Keywords: carbon nanotubes, nanocomposites, modeling, entangled fibers, Monte Carlo, finite elements, distributions.

1 INTRODUCTION

Since their discovery in 1991, single walled carbon nanotubes (SWCNT) have been considered as ideal polymer matrices fillers due to their exceptional physical properties. Experimental and theoretical results have shown that Young's moduli of SWCNT's are approximately 1 TPa depending on the diameter size and chirality [1-3], and a thermal conductivity of 6000 W/mK [4]. Despite these nanotube properties, several researchers have reported experiments with a modest improvement of the elastic and thermal properties of polymer nanocomposites (PNC) [5,6]. On the other hand, other experimentalists have reported a substantial increase in the effective properties [7,8]. In this context it has been postulated that nanotube alignment, dispersion, tube geometry, and load transfer properties are factors that can significantly affect the mechanical and thermal properties of PNC's [7,9].

In recent years, several efforts have been made to model the physical properties of PNC's. Various analytical and numerical techniques have been used to determine their effective properties ranging from the atomistic scale up to the continuum level. Odegard et al. [10] have presented an equivalent-continuum method to obtain an effective continuum straight fiber that includes interface interaction for a fixed value of nanotube length and diameter. This fiber model has been incorporated in the Mori-Tanaka (MT) approach for computing the effective properties of the composite assuming perfect bonding. Seidel and Lagoudas [11] have also obtained the SWCNT effective continuum fiber properties using a composite cylinder micromechanics approach. An interesting multiscale technique, called a structural mechanics approach, has been used by Li and Chou in [12]. This approach has also assumed a 3D RVE with straight nanotube geometry. Fisher et al. [13] were the first to study the effect of carbon nanotube waviness in the final effective properties by means of sinusoidal nanotube shape. However, the model does not take into account nanotube dispersion.

A more realistic approach would involve a model incorporating nanotube morphology in it. Recent experiments reveal that microscope images can be used to extract statistical information of nanotube morphology. In the work done in [14], atomic force microscope (AFM) images were used to measure individual nanotube lengths. It was found that the Weibull distribution was the best fit for the statistical behavior of SWCNT lengths. A similar study was made in [15], but in this case, the authors proposed a lognormal distribution for lengths and an experimental histogram for nanotube diameters. Clearly, the use of this information appears to be important in the modeling of PNC's.

Certain studies have already been made with the incorporation of nanotube geometric statistics. Thostenson and Chou [16] used diameter distributions functions for the case of MWCNT composites but the nanotube was still considered straight. A similar approach was made in [17].

They incorporated orientation, as well as aspect ratio distributions in the MT method. In this model the final properties are drastically changed when accounting for the aspect ratio distribution. Nevertheless, straight nanotube geometry was assumed. It appears that simultaneous accounting for the nanotube morphology and the dispersion characteristics has not been included in the above mentioned models. In this paper an attempt to address this aspect is made. It first presents the generation of random microstructures with the incorporation of nanotube morphology statistical information. Then, an embedded fiber finite element (EFFE) approach is presented as a tool to obtain microstructure effective properties. Finally, Monte Carlo simulations are conducted to derive useful statistics of the computed effective physical properties.

2 RANDOM MICROSTRUCTURE GENERATOR

It is known from experimental images that nanotubes inside the matrix do not have a fixed length and diameter; in fact, they can be defined as statistical entities. Thus, incorporating the nanotube length and diameter statistical distribution into the model can lead to a more realistic material representation and consequently the model would require less input parameters.

To simplify the geometry, each individual nanotube is treated as a one dimensional fiber that lies in a two-dimensional space. A representative volume element (RVE) of a given size hosts all the fibers. The number of fibers inside each generated RVE depends on the desired nanotube volume fraction, nanotube length and diameter distributions. To this end, the length and diameter distributions reported in the work by Wang et al. [14] and Ziegler et al. [15] are incorporated into the microstructure generation procedure. Therefore, the length and diameter of each fiber in the microstructure is one realization of the reported distributions. The nanotube length is bounded to a possible maximum and minimum value of 500 and 20 nm respectively. A linear relation between θ_{max} (maximum angle of deviation) and nanotube length is used. This choice is based on the fact that longer nanotubes are more likely than short ones to be curved. In this regard, each fiber consists of 11 nodes with its corresponding 10 segments regardless of their length. This means that the segment length l, run from 2 nm to 50 nm, as the nanotube length limits are set to 20 nm and 500 nm. The first node is randomly generated in the RVE space. The second node is also randomly generated but adjusted to be exactly at a distance l from the first node. From the third node to the 11th, the position of the i-th node is calculated using coordinate transformation resulting in the following expression,

$$\begin{bmatrix} x_{i+1} \\ y_{i+1} \end{bmatrix} = \begin{bmatrix} x_i \\ y_i \end{bmatrix} + \begin{bmatrix} \cos(\phi) & -\sin(\phi) \\ \sin(\phi) & \cos(\phi) \end{bmatrix} \begin{Bmatrix} l\cos(\theta) \\ l\sin(\theta) \end{Bmatrix}, \qquad (1)$$

where the angle ϕ represents the inclination of the previous segment (the segment formed by the nodes i-1 and i) with respect to the global coordinate system x-y and the angle θ is the angle between the segment being generated and the previous one (see Figure 1). In this generation process the value of θ is one realization of the angle of deviation PDF.

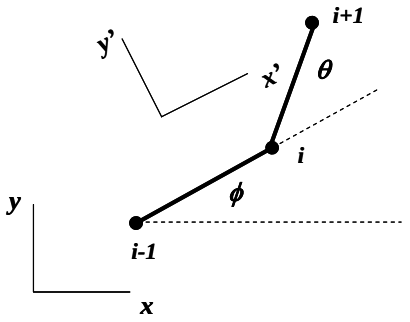

Figure 1. Coordinate transformation angles.

An example of a typical digitally generated random microstructure is shown in Figure 2 (a). Note the morphology similarity when compared to an actual nanocomposite image shown in Figure 2 (b).

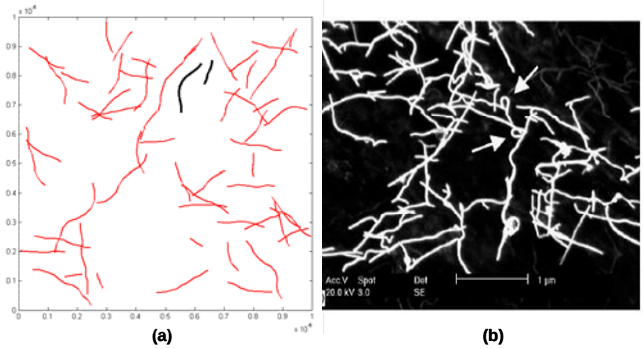

Figure 2. (a) One random microstructure realization. (b) Actual nanocomposite image from **[18]**

3 THE EMBEDDED FIBER FINITE ELEMENT METHO (EFFEM)

Several researchers have used FEM to calculate effective nanocomposite properties in many different geometry configurations[9]. However, in all of these studies, the representative volume element (RVE) used contains only one nanotube, leading to a relatively simple three-dimensional (3D) geometry to mesh.

In the present approach a more complex two-dimensional (2D) geometry is generated. Consequently, the mesh generation of the random microstructures will become a quite complex task even if the nanotubes are considered as one-dimensional (1D) elements. If it is desired to compute statistics of the effective nanocomposite properties using a Monte Carlo (MC) type finite element scheme, this model would be impractical if human intervention is required for the mesh generation process. One way to mitigate this problem is to use 1D line elements embedded in 2D quadrilateral elements.

The embedding procedure basically involves relating, by means of constraints, the 2D element degrees of freedom (dof's) with the 1D element dof's to be embedded using an expression of the form

$$[\mathbf{k}] = [\mathbf{T}]^T [\mathbf{k}'] [\mathbf{T}], \quad (2)$$

where $[\mathbf{k}']$ and $[\mathbf{T}]$ are the 1D fiber stiffness matrix and the constrained transformation matrix. Note that, this equation remains the same regardless of the physical problem analyzed, only the matrices dimensions change. Moreover, the final expression for the equivalent 2D element is

$$[\mathbf{K}]_{eqv} = [\mathbf{k}]_{Q4} + \sum_{i=1}^{n} [\mathbf{k}]_i , \quad (3)$$

where n is the total number of fibers inside the 2D element and the matrix $[\mathbf{k}]_{Q4}$ is the 2D element stiffness matrix. A rigorous derivation of the embedding process can be found in [19].

According to the study performed in [19], the EFFEM resemble the behavior of an orthotropic material when only one fiber is present. Thus, it can be defined as a complex homogenization method. Moreover, the accuracy of the computed effective properties depends drastically on the mesh sized. To illustrate this process, one random microstructure is generated and solved. Figure 3 and Figure 4 show the microstructure displacement and temperature contours, respectively. Clearly, the contours are refined around the fibers in the case of a finer mesh and thus yield a better estimate of the effective microstructure property (Young's modulus and thermal conductivity).

4 MODELING RESULTS: EXPERIMENTAL COMPARISON

It is worthy to compare the present approach results with experimental data towards validating its performance. To this aim, nanocomposite elastic modulus and thermal conductivity are the material physical properties used in this comparison. For the case of elastic modulus, the study done by Gonjy et al. [20] is chosen as reference. The proposed model requires volumetric content, thus [1] is followed to compute the weight-volume conversion. Figure 5 presents the simulation results vis-à-vis the experimental data.

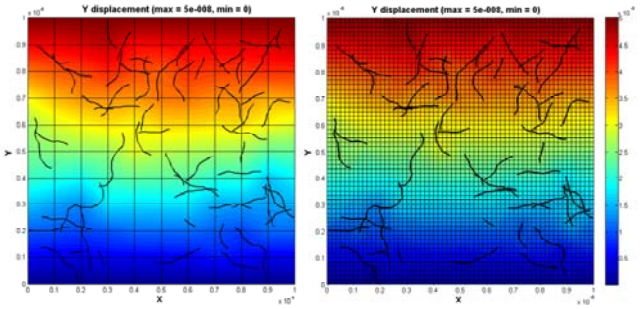

Figure 3. Microstructure vertical disp. contour: (Left) Mesh of 10X10 divisions. (Right) Mesh of 60X60 divisions.

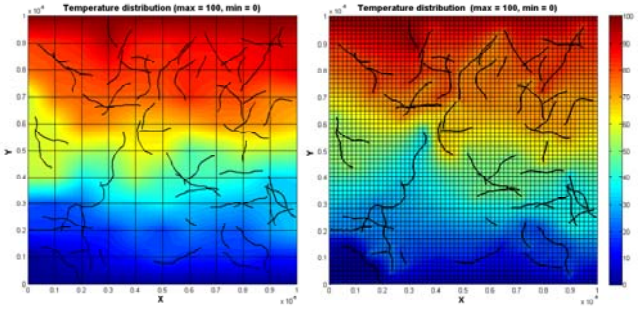

Figure 4. Microstructure temperature contour: (Left) Mesh of 10X10 divisions. (Right) Mesh of 60X60 divisions.

The modeling results are also compared with the experimental thermal properties reported in [21]. In this work, polyethylene/SWNT composites were experimentally tested to obtain the composite thermal conductivity. Preliminary MC runs indicated that using a SWNT thermal conductivity of 2000 W/m°C resulted in values that extremely over-estimated the experimental data. This can be attributed to the fact that thermal surface resistance has not been taken into account. Furthermore, the study done by Xue [22] indicated that the introduction of this resistance can reduce the conductivity in several orders of magnitude. Making use of this model, an effective thermal conductivity of 25 W/m°C is chosen to perform the simulations. The MC results are compared to the experimental values and they are shown in Figure 6.

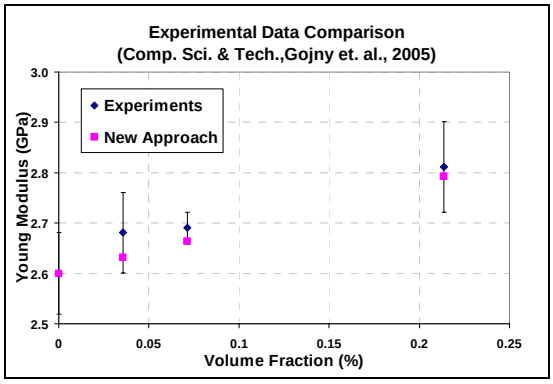

Figure 5. Experimental comparison: mechanical data.

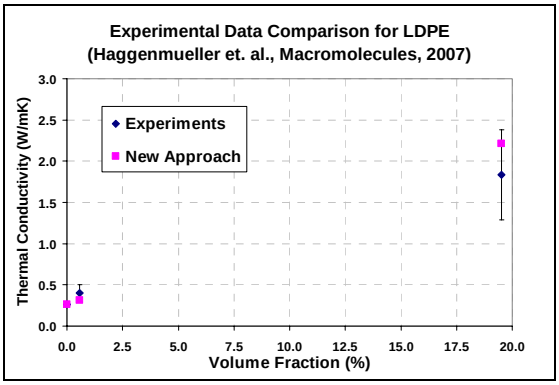

Figure 6. Experimental comparison: thermal data.

5 CONCLUSIONS

This paper has examined the nanotube dispersion and morphology effect on elastic and thermal nanocomposites properties. For this purpose, an approach to generate random microstructures has been developed with the incorporation of statistical distributions of nanotube length and diameters. Next, the embedded fiber finite element method (EFFEM) has been used to compute the microstructure effective properties. Then, the final nanocomposite properties have been calculated using a Monte Carlo scheme. Clearly, this approach has the quite appealing feature of requiring only a regular grid for the FE mesh, circumventing the time consuming human effort required for generating ultra fine meshes. The simulations results have been validated by comparison with experimental data for both physical properties.

REFERENCES

[1] R. Byron Pipes, S.J.V. Frankland, P. Hubert, and E. Saether, *Composites Science and Technology*, vol. 63, Aug. 2003, pp. 1349-1358.

[2] V.N. Popov, V.E. Van Doren, and M. Balkanski, *Solid State Communications*, vol. 114, Apr. 2000, pp. 395-399.

[3] E. Saether, S.J.V. Frankland, and R.B. Pipes, *Composites Science and Technology*, vol. 63, Aug. 2003, pp. 1543-1550.

[4] S. Berber, Y. Kwon, and D. Tomanek, *Physical Review Letters*, vol. 84, May. 2000, p. 4613.

[5] P.M. Ajayan, L.S. Schadler, C. Giannaris, and A. Rubio, *Advanced Materials*, vol. 12, 2000, pp. 750-753.

[6] A. Moisala, Q. Li, I. Kinloch, and A. Windle, *Composites Science and Technology*, vol. 66, Aug. 2006, pp. 1285-1288.

[7] W. Chen and X. Tao, *Applied Surface Science*, vol. 252, Mar. 2006, pp. 3547-3552.

[8] F.H. Gojny, M.H. Wichmann, B. Fiedler, I.A. Kinloch, W. Bauhofer, A.H. Windle, and K. Schulte, *Polymer*, vol. 47, Mar. 2006, pp. 2036-2045.

[9] S. Namilae and N. Chandra, *Journal of Engineering Materials and Technology*, vol. 127, Apr. 2005, pp. 222-232.

[10] G.M. Odegard, T.S. Gates, K.E. Wise, C. Park, and E.J. Siochi, *Composites Science and Technology*, vol. 63, Aug. 2003, pp. 1671-1687.

[11] G.D. Seidel and D.C. Lagoudas, *Mechanics of Materials*, vol. 38, 2006, pp. 884-907.

[12] C. Li and T. Chou, *Journal of nanoscience and nanotechnology*, vol. 3, Oct. 2003, pp. 423-30.

[13] F.T. Fisher, R.D. Bradshaw, and L.C. Brinson, *Composites Science and Technology*, vol. 63, Aug. 2003, pp. 1689-1703.

[14] S. Wang, Z. Liang, B. Wang, and C. Zhang, *Nanotechnology*, vol. 17, 2006, pp. 634-639.

[15] K.J. Ziegler, U. Rauwald, Z. Gu, F. Liang, W. Billups, R.H. Hauge, and R.E. Smalley, *Journal of Nanoscience and Nanotechnology*, vol. 7, Aug. 2007, pp. 2917-2921.

[16] E.T. Thostenson and T. Chou, *Journal of Physics D: Applied Physics*, vol. 36, 2003, pp. 573-582.

[17] B. Jiang, C. Liu, C. Zhang, B. Wang, and Z. Wang, *Composites Part B: Engineering*, vol. 38, Jan. 2007, pp. 24-34.

[18] J. Loos, A. Alexeev, N. Grossiord, C.E. Koning, and O. Regev, *Ultramicroscopy*, vol. 104, Sep. 2005, pp. 160-7.

[19] M. Esteva, "Hybrid Finite Elements Nanocomposite Characterization by Stochastic Microstructuring," Rice University, PhD Thesis, Department of Mechanical Engineering, 2008.

[20] F.H. Gojny, M.H. Wichmann, B. Fiedler, and K. Schulte, *Composites Science and Technology*, vol. 65, Dec. 2005, pp. 2300-2313.

[21] R. Haggenmueller, C. Guthy, J. Lukes, J. Fischer, and K. Winey, *Macromolecules*, vol. 40, Apr. 2007, pp. 2417-2421.

[22] Q.Z. Xue, *Nanotechnology*, vol. 17, 2006, pp. 1655-1660.